Tetrahedron 65 (2009) 8714–8721

Contents lists available at ScienceDirect

Tetrahedron

journal homepage: www.elsevier.com/locate/tet

Addition of kinetic boron enolates generated from β-alkoxy methyl ketones to aldehydes. Density functional theory calculations on the transition structures

Luiz C. Dias [a,*], Sávio M. Pinheiro [a], Vanda M. de Oliveira [a], Marco A.B. Ferreira [a], Cláudio F. Tormena [a], Andrea M. Aguilar [b], Julio Zukerman-Schpector [c], Edward R.T. Tiekink [c]

[a] Institute of Chemistry, University of Campinas, UNICAMP, PO Box 6154, 13084-971 Campinas, SP, Brazil
[b] Universidade Federal de São Paulo, UNIFESP, Campus Diadema, Departamento de Ciências Exatas e da Terra, R. Prof. Artur Ridel, 275, 09972-270 Diadema, SP, Brazil
[c] Universidade Federal de São Carlos, LaCrEMM-DQ, CP 676, 13565-905, São Carlos-SP, Brazil

ARTICLE INFO

Article history:
Received 9 June 2009
Received in revised form 17 August 2009
Accepted 17 August 2009
Available online 21 August 2009

Keywords:
Aldol reactions
Boron enolates
Theoretical calculations
Natural bond orbital analysis
1,5-Stereoinduction

ABSTRACT

Herein we report that good to excellent levels of 1,5-*anti* stereoinduction are obtained in boron enolate aldol reactions of 1,2-*syn* β-alkoxy methyl ketones with achiral aldehydes, when the β-alkoxy protecting group is part of a benzylidene acetal. We have also investigated the effects of the ligands on boron, the α-, β-, and γ-substituents and the β-alkoxy protecting group on the boron enolates, using density functional theory (B3LYP) and Møller–Plesset perturbation theory (MP2) calculations.

1. Introduction

The aldol reaction of the kinetic boron enolates of methyl ketones is a powerful method for C–C bond construction.[1] The boron enolates generated from α-methyl methyl ketones need the use of chiral ligands on boron in order to afford useful levels of 1,4-*syn* asymmetric induction.[2] On the other hand, the use of boron enolates of β-alkoxy methyl ketones affords the corresponding aldol products with moderate to high levels of 1,5-*anti* stereoinduction.[1] The first report on 1,5-*anti* stereoinduction in boron enolate aldol reactions of β-alkyloxy methyl ketones was described by Masamune and co-workers[3] in 1989. More recently, the research groups of Paterson,[4] Evans,[5] Dias,[6] and Goodman[7] made very important contributions. The levels of selectivity are heavily dependent on the nature of the β-alkoxy substituent and high degrees of 1,5-*anti* selectivities are obtained when the β-alkoxy protecting group is an alkyloxy group, a benzyloxy group (OBn, OPMB) or part of a benzylidene acetal.[4–9] Usually, the use of a β-silicon protecting group gives little or no selectivity, with a few exceptions.[6,10]

In continuation of our efforts to understand the factors controlling the 1,5-stereoinduction in these boron-mediated aldol reactions, we wish to describe here the use of chiral α,β-disubstituted and α,β,γ-trisubstituted methyl ketones.[11] The scope of the reaction was explored using methyl ketones with *tert*-butyldimethylsilyl (TBS), *p*-methoxybenzyl (PMB) as well as with benzylidene acetal protecting groups at the β-position.

2. Results and discussion

Our studies began by investigating the aldol reactions of 1,2-*syn* disubstituted methyl ketones **1** and **5**, containing a TBS protected hydroxyl group at the β-position, using $(c\text{-Hex})_2BCl/Et_3N$ in Et_2O for enolization (Scheme 1). Initially, we examined the aldol reaction of the less-substituted boron enolate formed from α,β,γ-trisubstituted methyl ketone **1** with aldehyde **2a**, which gave a 52:48 mixture of 1,5-*anti* and 1,5-*syn* aldol adducts **3** and **4**, respectively, in 79% yield.[12]

As shown in Scheme 1, the boron-mediated aldol reaction of the boron enolate prepared from 1,2-*syn* methyl ketone **5** showed only modest 1,5-stereoinduction upon addition of isobutyraldehyde (**2b**) to give a 70:30 mixture of 1,5-*anti* and 1,5-*syn* aldol adducts **6** and **7**, respectively, in 69% yield.[12,13] These findings with β-OTBS protecting groups are in agreement with literature results.[6,10]

Based on these results, we decided to explore the influence of a *p*-methoxybenzyl (PMB) group at the β-position in 1,2-*syn* methyl ketone **8** in reactions with aldehydes **2b–f** (Scheme 2 and Table 1).

* Corresponding author. Fax: +55 19 3521 3023.
E-mail address: ldias@iqm.unicamp.br (L.C. Dias).

0040-4020/$ – see front matter © 2009 Elsevier Ltd. All rights reserved.
doi:10.1016/j.tet.2009.08.042

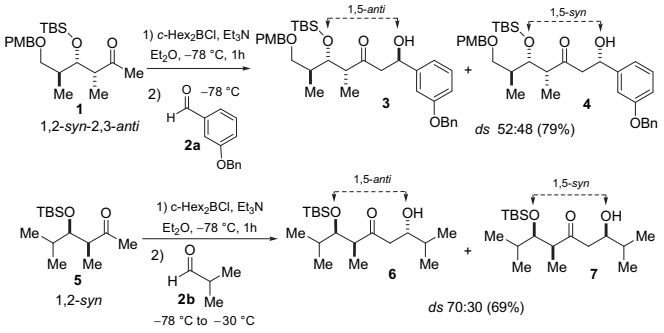

Scheme 1. Aldol reactions of the boron enolates generated from 1,2-*syn* β-alkoxy methyl ketones **1** and **5**.

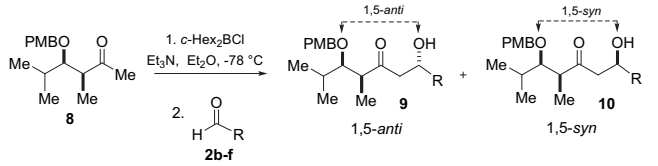

Scheme 2. Aldol reactions of the boron enolate generated from 1,2-*syn* β-alkoxy methyl ketone **8**.

Table 1
Aldol reactions of the boron enolate generated from methyl ketone **8**

Entry	Aldehyde (R)	ds[a] 1,5-*anti*/1,5-*syn*	Yield[b] (%)
1	**2b**, ^{i}Pr	53:47	88
2	**2c**, Et	67:33	90
3	**2d**, Ph	56:44	88
4	**2e**, *p*-MeOC$_6$H$_4$	50:50	94
5	**2f**, *p*-NO$_2$C$_6$H$_4$	67:33	82

[a] Diastereoselectivity was determined by ^{1}H and ^{13}C NMR analysis of the crude mixture of products.
[b] Combined yields for both 1,5-*syn* and 1,5-*anti* isomers after purification by flash column chromatography.

Surprisingly, the reactions presented in Scheme 2 and Table 1 resulted in low levels of diastereoselectivities favoring the corresponding 1,5-*anti* aldol adducts. In contrast to what was expected, the aldol addition of methyl ketone **8** showed that the stereoinduction from the β-alkoxy stereocenter is almost nonexistent. In addition, we believe that the α-methyl stereocenter exhibited a modest, intrinsic 1,4-*syn* stereoinduction. The relative stereochemistries for the major products **6** (Scheme 1) and **9b** (R=^{i}Pr) (Scheme 2) were assigned by transformation to the corresponding diols after removal of the TBS and PMB protecting groups, respectively, whose spectroscopic properties compared very well with literature data (see Supplementary data for additional details).[13]

We next examined the use of 1,2-*syn* methyl ketones containing a β-alkoxy substituent as a part of a benzylidene acetal. It should be noted that we tested a new experimental procedure for the aldol reactions of methyl ketones **11** (Scheme 3) and **17** (see Scheme 5). We found out that there is no need to wait additional time for the enolization and the aldehyde is added immediately after addition of (*c*-Hex)$_2$BCl and Et$_3$N to a solution of the corresponding methyl ketone in Et$_2$O as solvent at −78 °C. This leads to better results in terms of yields when compared with the normal enolization procedure, although the levels of diastereoselectivities are the same. Following this protocol, aldol reactions of 1,2-*syn* methyl ketone **11**, lacking the methyl group in γ-position relative to the carbonyl group, with aldehydes **2b**–**g**, at −78 °C, provided the corresponding 1,5-*anti* (**12b**–**g**) and 1,5-*syn* (**13b**–**g**) aldol adducts (Scheme 3, Table 2).[12] The boron-mediated aldol reactions of methyl ketone **11** were found to proceed with good yields and good levels of remote 1,5-*anti* stereoinduction. The best selectivity was observed with *p*-methoxybenzaldehyde (entry 4, 1,5-*anti*/1,5-*syn*=87:13).

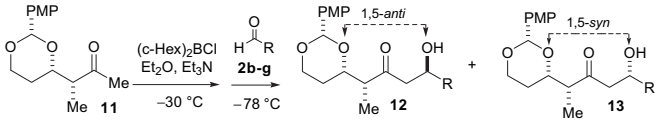

Scheme 3. Aldol reactions of the boron enolate prepared from 1,2-*syn* β-alkoxy methyl ketone **11**.

Table 2
Aldol reactions of the boron enolate generated from methyl ketone **11**

Entry	Aldehyde (R)	Solvent	ds[a] 1,5-*anti*/1,5-*syn*	Yield[b] (%)
1	**2b**, ^{i}Pr	Et$_2$O	86:14	83
2	**2c**, Et	Et$_2$O	80:20	84
3	**2d**, Ph	Et$_2$O	86:14	95
4	**2e**, *p*-MeOC$_6$H$_4$	Et$_2$O	87:13	82
5	**2f**, *p*-NO$_2$C$_6$H$_4$	Et$_2$O/CH$_2$Cl$_2$	80:20	52
6	**2g**, C(Me)=CH$_2$	Et$_2$O	85:15	67

[a] Diastereoselectivity was determined by ^{1}H and ^{13}C NMR analysis of the crude mixture of products.
[b] Combined yields for both 1,5-*syn* and 1,5-*anti* isomers after purification by flash column chromatography.

The 1,5-*anti* relationship for aldol adduct **12e** (R=*p*-MeOC$_6$H$_4$) was confirmed by a single-crystal X-ray diffraction analysis, as shown in Figure 1.[14]

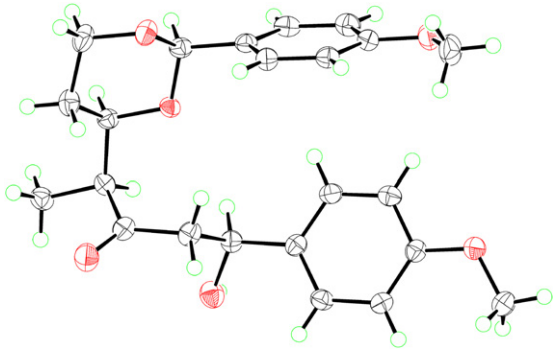

Figure 1. ORTEP3 diagram of the single-crystal X-ray structure of aldol adduct **12e**.[14]

The intrinsic facial selectivity of the boron enolate generated from α,β,γ-trisubstituted methyl ketone **14** was investigated before in our laboratories.[6f] For this purpose, we reacted the kinetic boron enolate generated from **14** with achiral aromatic, olefinic, and aliphatic aldehydes. We were delighted to find that this reaction led to the formation of 1,5-*anti* products **15** as the major isomers (up to >95:5 diastereoselectivity) (Scheme 4 and Table 3).[6f,12] These studies showed a remarkable influence of the resident β-alkoxy and γ-methyl stereocenters on the stereochemical course of these aldol reactions.[6]

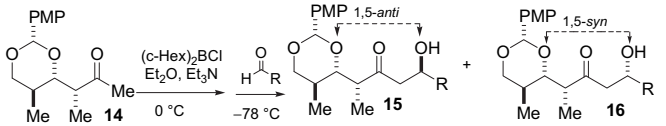

Scheme 4. Aldol reactions of the boron enolate prepared from 1,2-*syn* β-alkoxy methyl ketone **14**.[6f]

The configurational assignment of the major isomer as 1,5-*anti* was confirmed by a single-crystal X-ray structure determination of aldol adduct **15h** (R=Me).[6f]

With these encouraging results in hand, we next moved to investigate the aldol reactions of all-*syn*-trisubstituted methyl ketone **17**, where the absolute stereochemistry of the γ-stereocenter has been changed when compared with methyl ketone **14**. The aldol reactions of the 1,2-*syn* methyl ketone **17** with aldehydes **2b**–**k**

Table 3
Aldol reactions of the boron enolate generated from methyl ketone **14**[6f]

Entry	Aldehyde (R)	Solvent	ds[a] 1,5-*anti*/1,5-*syn*	Yield[b] (%)
1	**2a**, *m*-BnOC$_6$H$_4$	Et$_2$O	>95:05	82
2	**2b**, ^{i}Pr	Et$_2$O	>95:05	77
3	**2d**, Ph	Et$_2$O	>95:05	77
4	**2g**, C(Me)=CH$_2$	Et$_2$O	>95:05	75
5	**2h**, Me	Et$_2$O	>95:05	89

[a] Diastereoselectivity was determined by ^{1}H and ^{13}C NMR analysis of the crude mixture of products.
[b] Combined yields for both 1,5-*syn* and 1,5-*anti* isomers after purification by flash column chromatography.

were investigated using (*c*-Hex)$_2$BCl and Et$_3$N in Et$_2$O as solvent, to give the 1,5-*anti* and 1,5-*syn* aldol adducts **18** and **19**, respectively (Scheme 5, Table 4). As observed before, these boron-mediated aldol reactions were found to proceed with good yields and good degrees of remote 1,5-*anti* stereoinduction. Especially noteworthy is that this methyl ketone afforded lower levels of 1,5-*anti* diastereoselectivity when compared with methyl ketone **14**. These results clearly demonstrate, for the first time, that even the stereochemistry of the γ-stereocenter plays a significant role in the aldol addition reactions of these particular methyl ketones.

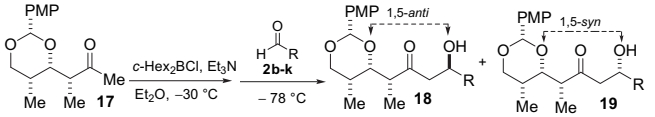

Scheme 5. Aldol reactions of the boron enolate prepared from 1,2-syn β-alkoxy methyl ketone **17**.

Table 4
Aldol reactions of the boron enolate generated from methyl ketone **17**

Entry	R	Solvent	ds[a] 1,5-*anti*/1,5-*syn*	Yield[b] (%)
1	**2b**, ^{i}Pr	Et$_2$O	86:14	97
2	**2c**, Et	Et$_2$O	88:12	51
3	**2d**, Ph	Et$_2$O	72:28	69
4	**2e**, *p*-MeOC$_6$H$_4$	Et$_2$O	86:14	70
5	**2f**, *p*-NO$_2$C$_6$H$_4$	Et$_2$O/CH$_2$Cl$_2$	>95:05	55
6	**2g**, C(Me)=CH$_2$	Et$_2$O	78:22	89
7	**2h**, Me	Et$_2$O	89:11	65
8	**2i**, CH$_2$CH$_2$Ph	Et$_2$O	90:10	94
9	**2j**, CH=CH$_2$	Et$_2$O	86:14	72
10	**2k**, *p*-FC$_6$H$_4$	Et$_2$O	86:14	59

[a] Diastereoselectivity was determined by ^{1}H and ^{13}C NMR analysis of the crude mixture of products.
[b] Combined yields for both 1,5-*syn* and 1,5-*anti* isomers after purification by flash column chromatography.

The 1,5-*anti* relative stereochemistry for aldol adducts **18b–k** was unambiguously established after conversion of **18b** (R=^{i}Pr) to the corresponding acetals **21** and **26** (Schemes 6 and 7). Selective reduction of **18b** performed very well to give the 1,3-*syn* diol **20** (83% yield). This was followed by treatment of **20** with Me$_2$C(OMe)$_2$ in the presence of catalytic amounts of CSA to give isopropylidene

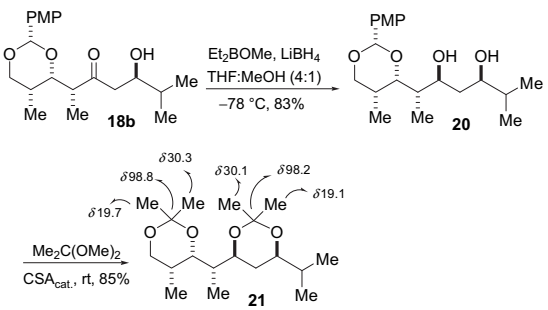

Scheme 6. Preparation of isopropylidene acetal **21**.

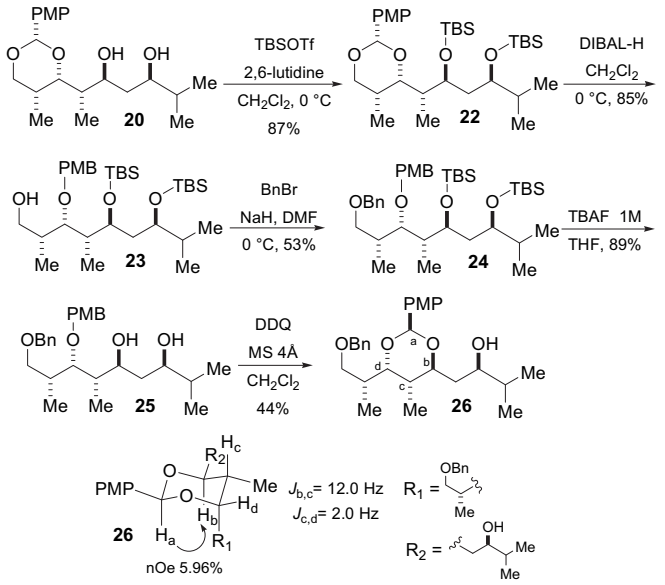

Scheme 7. Proof of stereochemistry for aldol adduct **18b**.

acetal **21** in 85% yield (Scheme 6). Analysis of the ^{13}C NMR spectra showed resonances at δ 19.1, 30.1, and 98.2 for **21**, as expected for a 1,3-*cis* acetonide.[15]

Having ascertained the relative stereochemistry for the 1,3-diol unit in diol **20**, we next moved to establish its relation with the stereocenters originally present in the boron enolate. Protection of **20** with TBSOTf gave the corresponding bis-silyl ether **22** in 87% yield, which, after treatment with DIBAL-H in CH$_2$Cl$_2$ provided primary alcohol **23** in 85% yield (Scheme 7). Alcohol **23** was protected as its benzyl ether (53%) and treated with TBAF to remove both TBS protecting groups to give diol **25** in 89% yield. Treatment of **25** with DDQ in CH$_2$Cl$_2$ in the presence of molecular sieves gave benzylidene acetal **26** in 44% yield (Scheme 7). Analysis of the ^{1}H NMR coupling constants for **26**, specifically J_{Hb-Hc}=12.0 Hz and J_{Hc-Hd}=2.0 Hz, together with the NOE interaction between Ha and Hb, proved that Ha, Hb, and Hc are all axial (Scheme 7), confirming the 1,5-*anti* stereochemistry for aldol adducts **18b–k**.

3. Aldol transition structures

3.1. Computational methods

All structures were fully optimized through the Gaussian03 program,[16] applying the B3LYP hybrid functional[17] and 6-31G(d,p) basis sets. For purposes of comparison, in some cases we calculated the single-point energies from these optimized structures applying the functional B3LYP hybrid in combination with 6-311++G(d,p) basis set, and the second-order Møller–Plesset perturbation theory (MP2)[18] in combination with 6-31+G(d,p). The relative energies for the transition structures were evaluated by single-point calculations (in Et$_2$O) from the gas-phase optimized geometries (PCM method).[19] The Cartesian coordinates are supplied in Supplementary data. In previous works, Paton and Goodman[7] observed that the single-point solvation energies and geometries were very similar to those obtained from a full optimization in solvents. The NBO delocalization energies (stabilizing energies calculated by second-order perturbation theory analysis) were calculated at the B3LYP/6-31G(d,p) level using NBO 5.0.[20,21] The frequency calculations for the observed transition structures were conducted to check for the presence of a single imaginary frequency and the corresponding eigenvector inspected to confirm the expected aldol reaction coordinate.

3.2. Simple 1,2-*syn* β-alkoxy methyl ketones

We were intrigued by the fact that 1,2-*syn* methyl ketone **8**, containing a β-alkoxy PMB protecting group, led to low levels of diastereoselection (Scheme 2, Table 1).

Recently, Paton and Goodman[7] published very interesting theoretical studies in order to explain the origins of the 1,5-*anti* asymmetric induction in boron-mediated aldol reactions of methyl ketones. They concluded that these reactions proceed via boat-like transition states and, based on Natural Bond Orbital analysis, proposed that a stabilizing formyl hydrogen bond favors the formation of the 1,5-*anti* aldol product.[7,20–22] Due to the lower basicity of the β-oxygen, it is proposed that silyl protecting groups prevent this formyl hydrogen bonding and led to the lower levels of observed selectivities. However, the lower basicity of the oxygen attached to the silicon may not be the only effect responsible for the observed lower selectivities as steric effects may play a very important role in controlling the observed sense of stereoinduction.[10a] We have observed that the use of a β-O^{t}Bu protecting group also gives the 1,5-*syn* isomers in similar levels of diastereoselectivities when compared with β-OTBS protecting groups.[6a,b]

Based on these results, we have performed theoretical calculations on the competing transition structures leading to both 1,5-*anti* and 1,5-*syn* aldol adducts. We based our work in the previous theoretical studies of Paton and Goodman[7] and only the boat-like transition structures were considered, as they are energetically more favorable because of the 1,3-diaxial type interactions present in the corresponding chair-like transition structures.[22]

Initially, we studied the simple aldol transition structures for α,β-dimethyl-β-methoxy dimethylboron enolate **8a** and acetaldehyde (Fig. 2). A summary of the low-energy structures is presented in Figure 2 (Fig. S1 in Supplementary data shows all the successfully optimized structures).

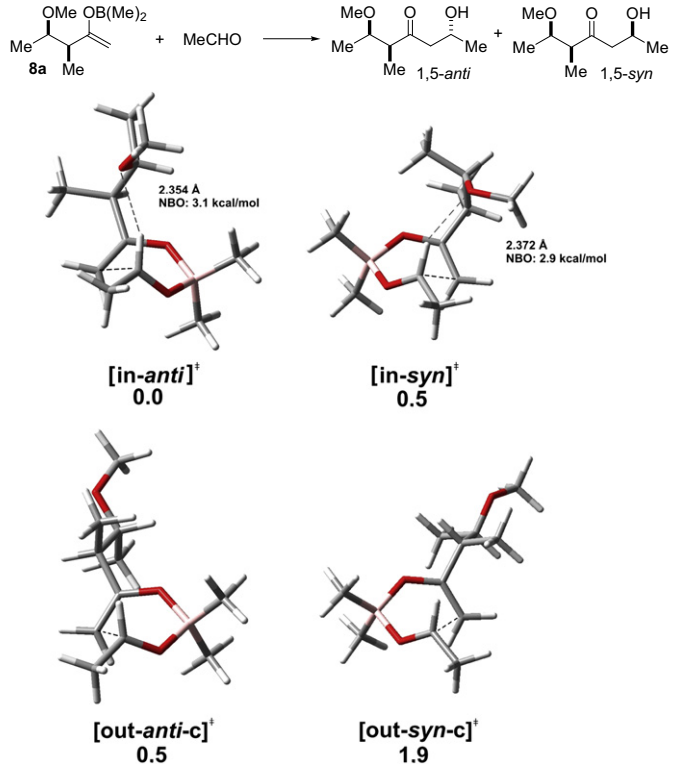

Figure 2. Aldol transition structures for α,β-dimethyl-β-methoxy dimethylboron enolate **8a** and acetaldehyde, leading to 1,5-*anti* and 1,5-*syn* aldol adducts (relative energies in kcal/mol calculated in Et_2O at B3LYP/6-31G(d,p)).

We have observed an energetic preference for the [in-*anti*] and [in-*syn*] conformers with a stabilizing formyl H-bond with delocalization energies of 3.1 and 2.9 kcal/mol, respectively (see Supplementary data for additional details).[23] This leads to a shorter O–H distance in the 1,5-*anti* transition structure (2.354 Å) as well as to a higher delocalization energy when compared with the 1,5-*syn* transition structure (2.372 Å).[7,20,21] Transition state [in-*anti*], which gives the 1,5-*anti* isomer, is lower in energy when compared with transition state [in-*syn*], which gives the 1,5-*syn* aldol adduct. This difference of 0.5 kcal/mol leads to a Boltzmann distribution of 8:2 at −78 °C, in favor of the 1,5-*anti* diastereoisomer. The $A_{1,3}$ type interaction of the α-Me group and one of the hydrogens of the enolate double bond seems to disfavor transition state [in-*anti*], while the steric interaction between the β-Me group in pseudo-axial position and one of the methyl ligands on boron disfavors transition state [in-*syn*].

These theoretical results are consistent with our experimental results using the boron enolate generated from methyl ketone **8** as they show a tendency to form the 1,5-*anti* aldol adduct as the major isomer (Scheme 1 and Table 1).

Although Paton and Goodman[7b] stated that a similar model also rationalizes the excellent levels of 1,4-*syn* selectivities observed in the reactions of α-methyl boron enolates, and correctly predicts the outcome of competition between 1,4- and 1,5-stereoinduction, where the latter dominates, we observed that this is not the case with α,β-*syn* disubstituted boron enolates of methyl ketones like **8**.

Due to the lower energy difference observed between transition states, it looks like this is the case of a *mismatched* relationship as there is a competition between 1,4-*syn* induction from the α-methyl stereocenter and 1,5-*anti* induction from the β-alkoxy stereocenter. This should also be the case with the β-OTBS methyl ketone **5** (Scheme 1).

At this point, we turned our attention to investigate the corresponding transition structures by replacing the β-Me group by a β-^{i}Pr group and the β-OMe substituent by a β-OBn group.

The lower energy transition states for the α-methyl-β-isopropyl-β-benzyloxy dimethylboron enolate **8b** are shown in Figure 3 (see in

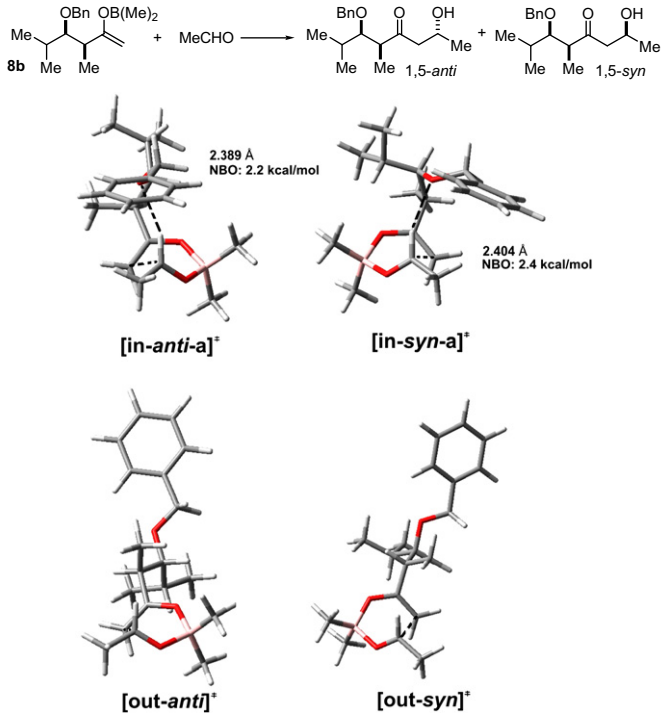

Figure 3. Aldol transition structures for α-methyl-β-isopropyl-β-benzyloxy dimethylboron enolate **8b** and acetaldehyde, leading to 1,5-*anti* and 1,5-*syn* aldol adducts (NBO energy in kcal/mol at B3LYP/6-31G(d,p)).

Supplementary data, Fig. S2 with all observed structures). The analysis of the relative energies of these transition structures (Table 5) proved that the density functional B3LYP shows relative energies favoring the corresponding [out-*anti*] transition structure, thus preventing the formyl H-bond. There was also a large energy difference between the competitive transition state [out-*anti*], of lower energy and which leads to 1,5-*anti* diastereoisomer, and [**out-*syn***] leading to 1,5-*syn* diastereoisomer, a situation which is inconsistent with our experimental results, as well as with the results described earlier by Paton and Goodman.[7]

Table 5
Relative energies (in kcal/mol calculated in Et_2O) of aldol transition structures for α-methyl-β-isopropyl-β-benzyloxy dimethylboron enolate **8b** and acetaldehyde

TS	B3LYP/6-31G (d,p)	B3LYP/6-311++g (d,p)//B3LYP/6-31G(d,p)	MP2/6-31+g (d,p)//B3LYP/6-31G(d,p)
in-*anti*-a	1.2	1.8	0.0
out-*anti*	0.0	0.0	2.3
in-*syn*-a	1.9	2.7	0.8
out-*syn*	1.3	1.3	4.2

The single-point energy calculation at the B3LYP/6-311++G(d,p) level did not lead to significant changes in the relative energies. However, the same single-point calculation using MP2/6-31+G(d,p) theory revealed now a lower energetic preference for the [in-*anti*-a] and [in-*syn*-a] conformers, which contain a stabilizing formyl H-bond. The O–H distance in the [in-*anti*-a] transition structure (2.389 Å) is shorter when compared with the [in-*syn*-a] transition structure (2.404 Å), with delocalization energies of 2.2 and 2.4 kcal/mol, respectively. In this case, the [in-*anti*-a], which gives the 1,5-*anti* isomer, is lower in energy when compared with transition state [in-*syn*-a], which gives the 1,5-*syn* aldol adduct. This difference of 0.8 kcal/mol leads to a Boltzmann distribution of 9:1 at −78 °C, in favor of the 1,5-*anti* diastereoisomer. The results presented in Figure 3 and Table 5 seem to be in agreement with our experimental results.

A possible explanation for these controversial results is on the employed DFT theory for calculation of the transition state relative energies. Recent publications show that for steric hindered systems the density functional B3LYP led to good quality geometries, but to poor quality relative energies.[7,24] Therefore, analysis of the competitive transition states that involves small differences in relative energies, provide discrepant quantitative results and it is necessary to use high level non-DFT methods to compute single-point energy from DFT-optimized structures, as recommended by Schreiner and co-workers.[24a] In this case, we believe that the steric energy between the eclipsed α-Me and β-^{i}Pr groups was super estimated in [in-*anti*-a] and [in-*syn*-a] conformers.

In order to obtain more information on these transition structures, we next examined the influence of dicyclohexyl substituents using the boron enolate **8c**. As shown in Table 6, the insertion of cyclohexyl groups do not generate significant differences in the relative energies of the observed transition states, independent on the theory level employed when compared to the previous case (Fig. 4, Table 5), in agreement with the observed results presented in Table 1.

Table 6
Relative energies (in kcal/mol calculated in Et_2O) of aldol transition structures for α-methyl-β-isopropyl-β-benzyloxy dicyclohexyl boron enolate **8c** and acetaldehyde

TS	B3LYP/ 6-31G(d,p)	B3LYP/6-311++g(d,p)// B3LYP/6-31G(d,p)	MP2/6-31+g(d,p)// B3LYP/6-31G(d,p)
in-*anti*-a	1.2	2.1	0.0
out-*anti*	0.0	0.0	2.6
in-*syn*-a	2.3	3.0	0.7
out-*syn*	1.4	1.2	4.9

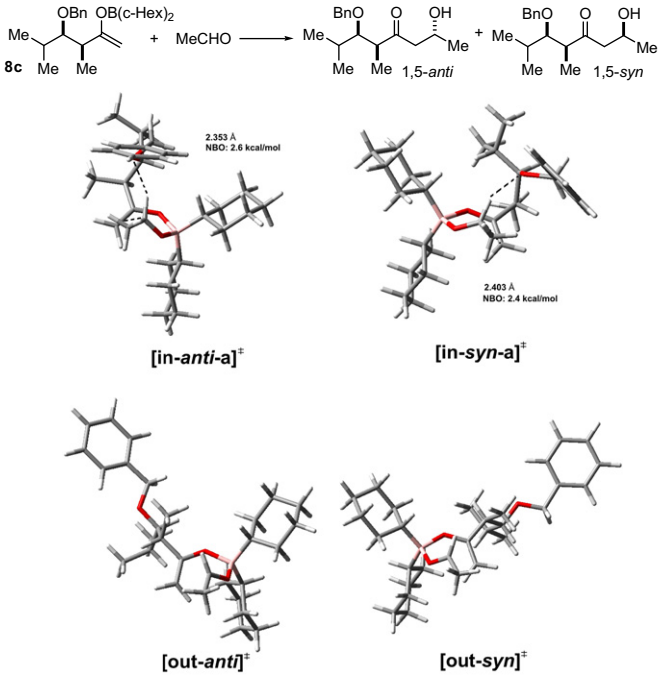

Figure 4. Aldol transition structures for α-methyl-β-isopropyl-β-benzyloxy dicyclohexyl boron enolate **8c** and acetaldehyde, leading to 1,5-*anti* and 1,5-*syn* aldol adducts (NBO energies in kcal/mol at B3LYP/6-31G(d,p)).

In these cases, the cyclohexyl groups are not responsible for the diastereodifferentiation, but they keep the ring in a rigid boat-like conformation, avoiding the 1,3-diaxial interactions between the boron and the ring substituents.

3.3. Boron enolates of β-benzylidene acetal-substituted methyl ketone

In the case of β-benzylidene acetal-substituted boron enolates, Paton and Goodman[7] observed that the favored transition structure has the six-membered acetal ring in a chair-like conformation, with the substituents in equatorial positions. The preferred 1,5-*anti* transition structure has the acetal oxygen oriented toward the formyl hydrogen.

*3.3.1. 1,2-syn-α-Methyl,β-alkoxy dimethylboron enolate (**8d**).* In order to better understand the results described in Schemes 3–5, we decided to examine the corresponding transition structures, starting with boron enolate **8d** (calculated for a more simple system in which the PMB group is replaced by a phenyl group) (Fig. 5).

Toward that end, as can be observed from Figure 7 and Table 5, different results were obtained depending on the employed theory level. Using B3LYP/6-31G(d,p) the [in-*syn*] transition state leading to 1,5-*syn* aldol adduct is lower in energy, although this is not the observed major product. The single-point energy calculation at the B3LYP/6-311++G(d,p) level led to the [in-*anti*] and [out-*anti*] low-energy transition structures. As noted earlier, the density functional B3LYP did not furnish an accurate determination of the relative energy.[7,24] The single-point analysis employing a higher theory level (MP2/6-31+G(d,p)) showed that only the transition states [in-*anti*] and [in-*syn*] containing a stabilizing hydrogen bond are lower in energy (Table 7). The O–H distance in the [in-*anti*] transition structure (2.332 Å) is shorter when compared with the [in-*syn*] transition structure (2.383 Å), with delocalization energies of 3.3 and 2.3 kcal/mol, respectively.

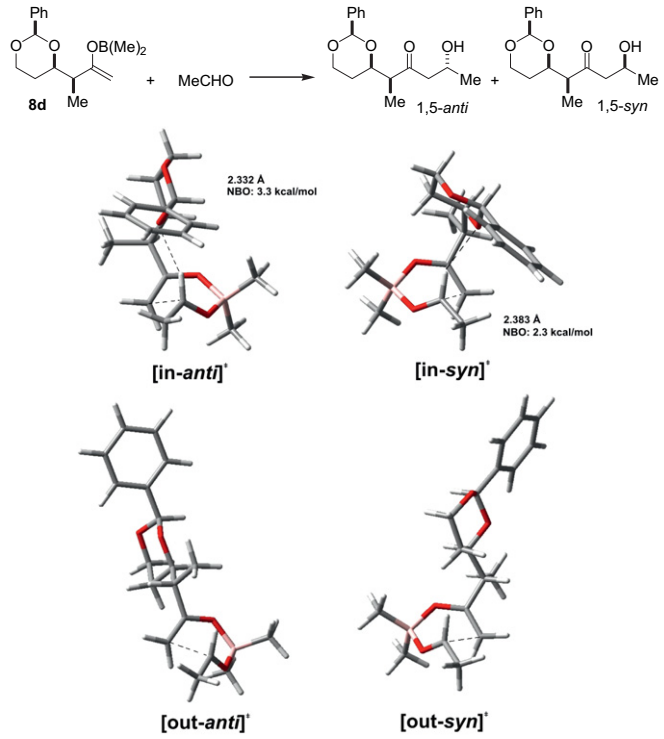

Figure 5. Aldol transition structures for 1,2-*syn*-α-methyl,β-alkoxy dimethylboron enolate **8d** and acetaldehyde, leading to 1,5-*anti* and 1,5-*syn* aldol adducts (NBO energies in kcal/mol at B3LYP/6-31G(d,p)).

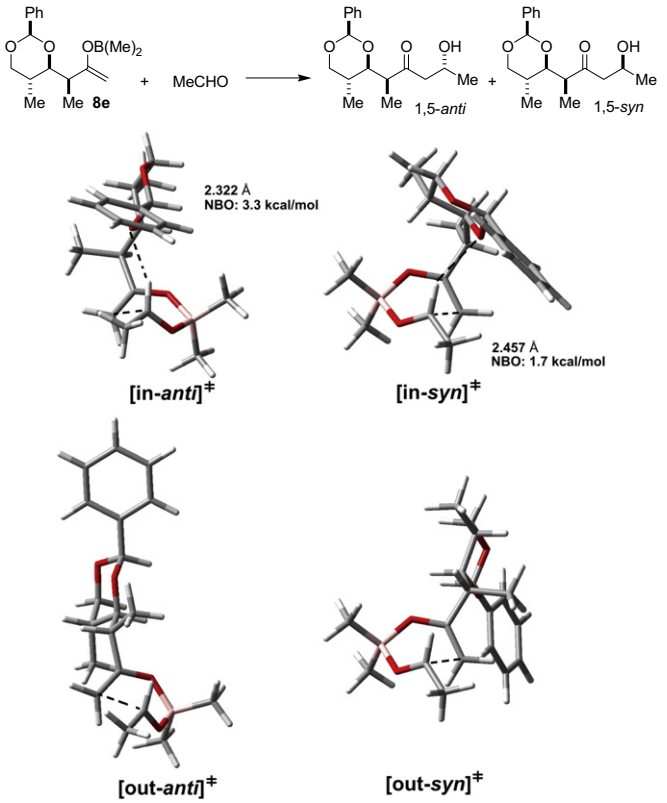

Figure 6. Aldol transition structures for 1,2-*syn*-2,3-*anti*-α,γ-methyl,β-alkoxy dimethylboron enolate **8e** and acetaldehyde, leading to 1,5-*anti* and 1,5-*syn* aldol adducts (NBO energies in kcal/mol at B3LYP/6-31G(d,p)).

In this case, the [in-*anti*], which gives the 1,5-*anti* isomer, is lower in energy (0.1 kcal/mol) when compared with transition state [in-*syn*], which gives the 1,5-*syn* aldol adduct.

This indicates a possible competition between 1,4- and 1,5-asymmetric induction, leading to a Boltzmann distribution of 6:4 at −78 °C, favoring the 1,5-*anti* diastereoisomers. These qualitative results are in accordance with our experimental results. Again, the $A_{1,3}$ type interaction of the α-Me group and the one of the hydrogens of the enolate double bond seems to disfavor transition state [in-*anti*], while steric interactions between the ligands on boron and the benzylidene acetal substituents disfavor transition state [in-*syn*] (Table 7).

Table 7
Relative energies (in kcal/mol calculated in Et_2O) of aldol transition structures for 1,2-*syn*-α-methyl,β-alkoxy dimethylboron enolate **8d** and acetaldehyde

TS	B3LYP/6-31G (d,p)	B3LYP/6-311++g (d,p)//B3LYP/6-31G(d,p)	MP2/6-31+g (d,p)//B3LYP/6-31G(d,p)
in-*anti*	0.2	0.2	0.0
out-*anti*	0.9	0.0	3.0
in-*syn*	0.0	0.7	0.1
out-*syn*	2.1	1.3	4.8

*3.3.2. 1,2-syn-2,3-anti-α,γ-Methyl,β-alkoxy dimethylboron enolate (**8e**).* We next moved to investigate the transition structures for α,β,γ-trisubstituted boron enolate **8e** (calculated for a simpler system in which the PMB group is replaced by a phenyl group, keeping the acetal ring in a chair-like conformation, with all bulky substituents in pseudo-equatorial positions) (Fig. 6, Table 8).

We have observed a preference for the transition structure [in-*anti*], independent on the theory level employed. The formyl hydrogen bond (H–O) is shorter in transition structure [in-*anti*] (2.332 Å) when compared with 2.457 Å observed for the [in-*syn*] transition structure, with delocalization energies of 3.3 and 1.7 kcal/mol, respectively.

Table 8
Relative energies (in kcal/mol calculated in Et_2O) of aldol transition structures for 1,2-*syn*-2,3-*anti*-α,γ-methyl,β-alkoxy dimethylboron enolate **8e** and acetaldehyde

TS	B3LYP/6-31G (d,p)	B3LYP/6-311++g (d,p)//B3LYP/6-31G(d,p)	MP2/6-31+g (d,p)//B3LYP/6-31G(d,p)
in-*anti*	0.0	0.0	0.0
out-*anti*	2.6	2.1	5.0
in-*syn*	1.9	2.7	2.3
out-*syn*	2.2	1.6	5.5

The 1,5-*anti* [in-*anti*] transition structure is 2.3 kcal/mol more stable than the 1,5-*syn* [in-*syn*], leading to a 10:0 Boltzmann distribution at −78 °C by using the MP2/6-31+G(d,p) single-point analysis. This result is in perfect agreement with our experimental observations. The high-energy difference of these conformers is probably due to the severe repulsive interactions between α and γ-methyl groups at the axial positions in transition structure [in-*syn*].

3.3.3. 1,2,3-syn-α,γ-Methyl,β-alkoxy boron enolate. Finally, we investigated the transition structure for α,β,γ-trisubstituted boron enolate **8f** (calculated for a simpler system in which the PMB group is replaced by a phenyl group) (Fig. 7, Table 9). Furthermore, the benzylidene acetal ring (see Supplementary data in Fig. S7 and Table S11, for additional information) shows a preference for a chair-like conformation with all bulky substituents in pseudo-equatorial positions and the γ-methyl group in a pseudo-axial position. The competitive transition structures are shown in Figure 7 (see Supplementary data in Fig. S8 and Table S13, for all the observed structures).

It is interesting to observe that the most stable transition state conformers are [out-*anti*-d] and [out-*syn*-c], and the conformers [in-*anti*] and [in-*syn*] containing a stabilizing hydrogen bond are

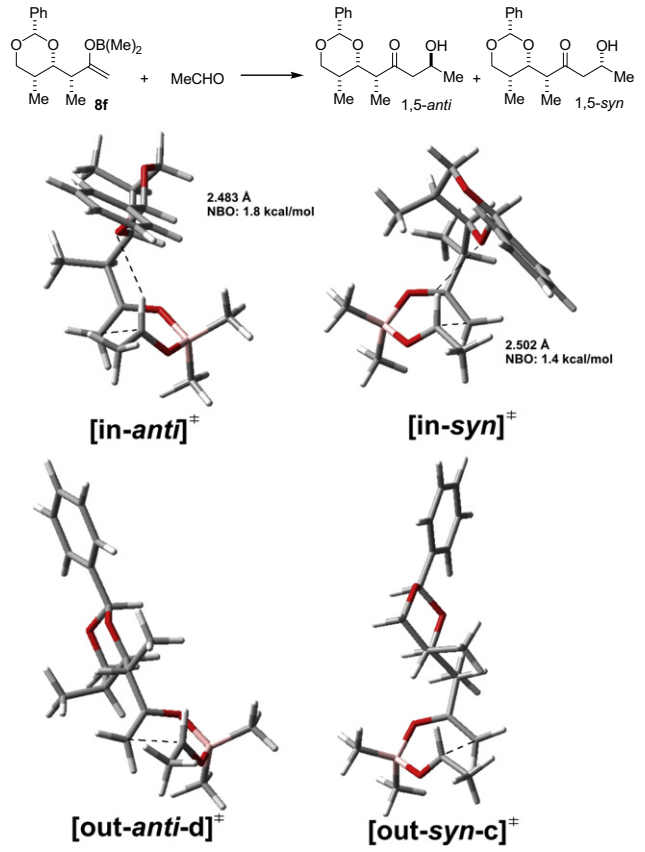

Figure 7. Aldol transition structures for all-*syn*-α,γ-methyl,β-alkoxy boron enolate **8f** and acetaldehyde, leading to 1,5-*anti* and 1,5-*syn* aldol adducts (NBO energies in kcal/mol at B3LYP/6-31G(d,p)).

Table 9
Relative energies (in kcal/mol calculated in Et_2O) of aldol transition structures for all-*syn*-α,γ-methyl,β-alkoxy boron enolate **8f** and acetaldehyde

TS	B3LYP/6-31G (d,p)	B3LYP/6-311++g (d,p)//B3LYP/6-31G(d,p)	MP2/6-31+g (d,p)//B3LYP/6-31G(d,p)
in-*anti*	2.3	2.4	0.5
out-*anti*-d	0.0	0.0	0.0
in-*syn*	3.2	4.2	0.8
out-*syn*-c	1.0	0.9	0.6

higher in energy, regardless of the theory level employed (Table 9). This is probably due to the severe steric interactions between the methyl groups in α and γ-positions as well as with the hydrogens of the enolate double bond in 1,5-*anti* [in-*anti*] transition state. There is also a higher steric interaction between the γ-methyl group and the ligands on boron in the transition state 1,5-*syn* [in-*syn*]. In fact, these steric interactions are reflected in the weaker formyl hydrogen bond (2.483 Å and 2.502483 Å) for [in-*anti*] and [in-*syn*], with low delocalization energies of 1.8 and 1.4 kcal/mol, respectively. The difference in energy of competitive transition states from the single-point at the MP2/6-31+G(d,p) led to a Boltzmann distribution of 8:2 at −78 °C in favor of the 1,5-*anti* diastereoisomers. These findings are in perfect agreement with our experimental results (Scheme 5, Table 4).

4. Conclusions

In summary, we have reported that the nature of the β-alkoxy substituent is critical in determining the level of induction and high selectivities obtained in aldol reactions of boron enolates of β-substituted methyl ketones when the β-alkoxy protecting group is part of a benzylidene acetal. The strong internal stereoinduction of the β-alkoxy stereocenter of the boron enolates dominates the overall stereochemical outcome of the corresponding aldol addition reactions, leading to the 1,5-*anti* products with high diastereoselectivities. Even with the use of α-methyl-β-alkoxy methyl ketones, the β-stereocenter plays a dominant role in determining the sense of 1,5-*anti* asymmetric induction. The examples presented in this work show that the levels of facial selection are dependent on the absolute stereochemistries of the chiral boron enolates. In order to gain insight on the stereochemical outcome of these aldol couplings, we have performed theoretical calculations on the kinetic boron enolates generated from β-alkoxy methyl ketones with acetaldehyde using density functional theory by means of B3LYP and ab initio MP2 method. The magnitude of the formyl hydrogen bond has been evaluated using NBO perturbation theory analysis. In some cases, different results were obtained depending on the employed theory level. Further studies in this direction, especially in order to stress the importance of a competing 1,4-*syn* induction are underway and will be described in due course.

Acknowledgements

We are grateful to FAEP-UNICAMP, FAPESP (Fundação de Amparo à Pesquisa do Estado de São Paulo), CNPq (Conselho Nacional de Desenvolvimento Científico e Tecnológico), and INCT-INOFAR Proc. CNPq 573.564/2008-6 for financial support. We thank also Prof. Carol H. Collins for helpful suggestions about English grammar and style and Prof. Jonathan M. Goodman for useful comments on the theoretical calculations.

Supplementary data

Spectroscopic data for the prepared compounds, crystallographic data for aldol **12e**, and Cartesian coordinates of all transition structures with gas-phase and solution-phase SCF absolute energies. Supplementary data associated with this article can be found in the online version, at doi:10.1016/j.tet.2009.08.042.

References and notes

1. (a) Dias, L. C.; Aguilar, A. M. *Chem. Soc. Rev.* **2008**, *37*, 451; (b) Dias, L. C.; Aguilar, A. M. *Quim. Nova* **2007**, *30*, 2007; (c) Cowden, C. J.; Paterson, I. *Org. React.* **1997**, *51*, 1; (d) Franklin, A. S.; Paterson, I. *Contemp. Org. Synth.* **1994**, *1*, 317; (e) Heathcock, C. H. In *Comprehensive Organic Synthesis*; Heathcock, C. H., Ed.; Pergamon: New York, NY, 1991; Vol. 2, p 181; (f) Kim, B. M.; Williams, S. F.; Masamune, S. In *Comprehensive Organic Synthesis*; Heathcock, C. H., Ed.; Pergamon: New York, NY, 1991; Vol. 2, p 239; (g) Evans, D. A.; Nelson, J. V.; Taber, T. R. *Top. Stereochem.* **1982**, *13*, 1; (h) Schetter, B.; Mahrwald, R. *Angew. Chem., Int. Ed.* **2006**, *45*, 7506; (i) Denmark, S. E.; Henke, B. R. *J. Am. Chem. Soc.* **1991**, *113*, 2177.
2. Yeung, K.-S.; Paterson, I. *Chem. Rev.* **2005**, *105*, 4237.
3. Blanchette, M. A.; Malamas, M. S.; Nantz, M. H.; Roberts, J. C.; Somfai, P.; Whritenour, D. C.; Masamune, S.; Kageyama, M.; Tamura, T. *J. Org. Chem.* **1989**, *54*, 2817.
4. (a) Paterson, I.; Oballa, R. M.; Norcross, R. D. *Tetrahedron Lett.* **1996**, *37*, 8581; (b) Paterson, I.; Goodman, J. M. *Tetrahedron Lett.* **1989**, *30*, 997; (c) Paterson, I.; Florence, G. J. *Tetrahedron Lett.* **2000**, *41*, 6935; (d) Paterson, I.; Gibson, K. R.; Oballa, R. M. *Tetrahedron Lett.* **1996**, *37*, 8585; (e) Paterson, I.; Collett, L. A. *Tetrahedron Lett.* **2001**, *42*, 1187.
5. (a) Evans, D. A.; Côté, B.; Coleman, P. J.; Connell, B. T. *J. Am. Chem. Soc.* **2003**, *125*, 10893; (b) Evans, D. A.; Coleman, P. J.; Côté, B. *J. Org. Chem.* **1997**, *62*, 788; (c) Evans, D. A.; Trotter, B. W.; Coleman, P. J.; Côté, B.; Dias, L. C.; Rajapakse, H. A.; Tyler, A. N. *Tetrahedron* **1999**, *29*, 8671.
6. (a) Dias, L. C.; Marchi, A. A.; Ferreira, M. A. B.; Aguilar, A. M. *J. Org. Chem.* **2008**, *73*, 6299; (b) Dias, L. C.; Marchi, A. A.; Ferreira, M. A. B.; Aguilar, A. M. *Org. Lett.* **2007**, *9*, 4869; (c) Dias, L. C.; Aguilar, A. M. *Org. Lett.* **2006**, *8*, 4629; (d) Dias, L. C.; Salles, A. G., Jr. *Tetrahedron Lett.* **2006**, *47*, 2213; (e) Dias, L. C.; Aguilar, A. M.; Salles, A. G., Jr.; Steil, L. J.; Roush, W. R. *J. Org. Chem.* **2005**, *70*, 10461; (f) Dias, L. C.; Baú, R. Z.; de Sousa, M. A.; Zukerman-Schpector, J. *Org. Lett.* **2002**, *4*, 4325.
7. (a) Paton, R. S.; Goodman, J. M. *Org. Lett.* **2006**, *8*, 4299; (b) Paton, R. S.; Goodman, J. M. *J. Org. Chem.* **2008**, *73*, 1253; (c) Goodman, J. M.; Paton, R. S. *Chem. Commun.* **2007**, 24.
8. (a) Tanimoto, N.; Gerritz, S. W.; Sawabe, A.; Noda, T.; Filla, S. A.; Masamune, S. *Angew. Chem., Int. Ed. Engl.* **1994**, *33*, 673; (b) Roush, W. R.; Bannister, T. D.; Wendt, M. D.; Jablonowski, J. A.; Scheidt, K. A. *J. Org. Chem.* **2002**, *67*, 4275;

(c) Arefolov, A.; Panek, J. S. *Org. Lett.* **2002**, *4*, 2397; (d) Arefolov, A.; Panek, J. S. *J. Am. Chem. Soc.* **2005**, *127*, 5596.
9. (a) Denmark, S. E.; Fujimori, S.; Pham, S. M. *J. Org. Chem.* **2005**, *70*, 10823; (b) Denmark, S. E.; Fujimori, S. *Synlett* **2001**, 1024; (c) Denmark, S. E.; Fujimori, S. *J. Am. Chem. Soc.* **2005**, *127*, 8971.
10. For a discussion of the coordinating abilities of various ether substituents, see: (a) Dias, L. C.; Ferreira, M. A. B.; Tormena, C. F. *J. Phys. Chem. A* **2008**, *112*, 232; (b) Reetz, M. T. *Acc. Chem. Res.* **1993**, *26*, 462; (c) Chen, X. N.; Hortellano, E. R.; Eliel, E. L.; Frye, S. V. *J. Am. Chem. Soc.* **1990**, *112*, 6130; (d) Mori, S.; Nakamura, M.; Nakamura, E.; Koga, N.; Morokuma, K. *J. Am. Chem. Soc.* **1995**, *117*, 5055; (e) Schreiber, S. L.; Shambayati, S.; Blake, J. F.; Wierschke, S. G.; Jorgensen, W. L. *J. Am. Chem. Soc.* **1990**, *112*, 697; (f) Beckmann, J.; Grabowsky, S. *J. Phys. Chem. A* **2007**, *111*, 2011.
11. (a) Evans, D. A.; Chapman, K. T. *Tetrahedron Lett.* **1986**, *27*, 5939; (b) Evans, D. A.; Chapman, K. T.; Carreira, E. M. *J. Am. Chem. Soc.* **1988**, *110*, 3560; (c) Dias, L. C.; de Oliveira, L. G.; Vilcachagua, J. D.; Nigsch, F. *J. Org. Chem.* **2005**, *70*, 2225; (d) Dias, L. C.; de Oliveira, L. G. *Org. Lett.* **2004**, *6*, 2587; (e) Dias, L. C.; de Oliveira, L. G.; de Sousa, M. A. *Org. Lett.* **2003**, *5*, 265.
12. (a) The ratios were determined by ^{1}H and ^{13}C NMR spectroscopic analysis of the unpurified product mixture; (b) All of the percentage values represent data obtained from at least three individual trials.
13. Compound **6** has been prepared by related studies using ethyl ketones instead of methyl ketones: Luke, G. P.; Morris, J. *J. Org. Chem.* **1995**, *60*, 3013.
14. ORTEP3 for Windows: Farrugia, L. J. *J. Appl. Crystallogr.* **1997**, *30*, 565.
15. (a) Rychnovsky, S. D.; Skalitzky, D. J. *Tetrahedron Lett.* **1990**, *31*, 945; (b) Evans, D. A.; Rieger, D. L.; Gage, J. R. *Tetrahedron Lett.* **1990**, *31*, 7099; (c) Tormena, C. F.; Dias, L. C.; Rittner, R. *J. Phys. Chem. A* **2005**, *109*, 6077; (d) Dias, L. C.; Giacomini, R. *Tetrahedron Lett.* **1998**, *39*, 5343; (e) Dias, L. C.; Diaz, G.; Ferreira, A. A.; Meira, P. R. R.; Ferreira, E. *Synthesis* **2003**, 603.
16. Gaussian03 program: Frisch, M. J.; Trucks, G. W.; Schlegel, H. B.; Scuseria, G. E.; Robb, M. A.; Cheeseman, J. R.; Montgomery, J. A., Jr.; Vreven, T.; Kudin, K. N.; Burant, J. C.; Millam, J. M.; Iyengar, S. S.; Tomasi, J.; Barone, V.; Mennucci, B.; Cossi, M.; Scalmani, G.; Rega, N.; Petersson, G. A.; Nakatsuji, H.; Hada, M.; Ehara, M.; Toyota, K.; Fukuda, R.; Hasegawa, J.; Ishida, M.; Nakajima, T.; Honda, Y.; Kitao, O.; Nakai, H.; Klene, M.; Li, X.; Knox, J. E.; Hratchian, H. P.; Cross, J. B.; Bakken, V.; Adamo, C.; Jaramillo, J.; Gomperts, R.; Stratmann, R. E.; Yazyev, O.; Austin, A. J.; Cammi, R.; Pomelli, C.; Ochterski, J. W.; Ayala, P. Y.; Morokuma, K.; Voth, G. A.; Salvador, P.; Dannenberg, J. J.; Zakrzewski, V. G.; Dapprich, S.; Daniels, A. D.; Strain, M. C.; Farkas, O.; Malick, D. K.; Rabuck, A. D.; Raghavachari, K.; Foresman, J. B.; Ortiz, J. V.; Cui, Q.; Baboul, A. G.; Clifford, S.; Cioslowski, J.; Stefanov, B. B.; Liu, G.; Liashenko, A.; Piskorz, P.; Komaromi, I.; Martin, R. L.; Fox, D. J.; Keith, T.; Al-Laham, M. A.; Peng, C. Y.; Nanayakkara, A.; Challacombe, M.; Gill, P. M. W.; Johnson, B.; Chen, W.; Wong, M. W.; Gonzalez, C.; Pople, J. A. *Gaussian 03, Revision E.01*; Gaussian: Wallingford, CT, 2004.
17. B3LYP hybrid functional: (a) Lee, C.; Yang, W.; Parr, R. G. *Phys. Rev. B* **1988**, *37*, 785; (b) Becke, A. D. *Phys. Rev. A* **1988**, *38*, 3098; (c) Becke, A. D. *J. Chem. Phys.* **1993**, *98*, 5648.
18. (a) Head-Gordon, M.; Pople, J. A.; Frisch, M. J. *Chem. Phys. Lett.* **1988**, *153*, 503; (b) Frisch, M. J.; Head-Gordon, M.; Pople, J. A. *Chem. Phys. Lett.* **1990**, *166*, 275; (c) Frisch, M. J.; Head-Gordon, M.; Pople, J. A. *Chem. Phys. Lett.* **1990**, *166*, 281; (d) Saebo, S.; Almlof, J. *Chem. Phys. Lett.* **1989**, *154*, 83.
19. (a) Miertus, S.; Scrocco, E.; Tomasi, J. *Chem. Phys.* **1981**, *55*, 117; (b) Mennucci, B.; Tomasi, J. *J. Chem. Phys.* **1997**, *106*, 5151.
20. Weinhold natural bond orbital (NBO 5.0) analysis: (a) Glendening, E. D.; Badenhoop, J. K., Reed, A. E.; Carpenter, J. E.; Bohmann, J. A.; Morales, C. N.; Weinhold, J. NBO 5.G compiled with Gaussian 03. (b) Weinhold, F. *J. Mol. Struct. (THEOCHEM)* **1997**, *398–399*, 181; (c) Weinhold, F. *Nature* **2001**, *411*, 539; (d) Schreiner, P. R. *Angew. Chem., Int. Ed.* **2002**, *41*, 3579; (e) Pophristic, V.; Goodman, L. *Nature* **2001**, *411*, 565.
21. Electronic structures of the transition states were studied using Weinhold natural bond orbital (NBO 5.0) analysis.
22. There are three possibilities of ring conformation for the transition structures of aldol reaction of boron enolate, but the boat-like transition structures are energetically more favorable because avoid the 1,3 diaxial interaction between enolate side chain and the ligand that is present in the chair-like structure. See Houk and Bernardi's works: (a) Li, Y.; Paddon-Row, M. N.; Houk, K. N. *J. Am. Chem. Soc.* **1988**, *110*, 3684; (b) Li, Y.; Paddon-Row, M. N.; Houk, K. N. *J. Org. Chem.* **1990**, *55*, 481; (c) Bernardi, A.; Capelli, A. M.; Gennari, C.; Goodman, J. M.; Paterson, I. *J. Org. Chem.* **1990**, *55*, 3576.
23. As suggested by Paton and Goodman (Ref. 7), we label these structures as 'in' and 'out' to signify whether the β–alkoxy substituent points in toward the approaching aldehyde (with a stabilizing formyl hydrogen bond), or out and away from the aldehyde (absence of a stabilizing formyl hydrogen bond).
24. (a) Schreiner, P. R.; Folkin, A. A.; Pascal, R. A.; Meijere, A. *Org. Lett.* **2006**, *8*, 3635; (b) Grimme, S. *Angew. Chem., Int. Ed.* **2006**, *45*, 4460; (c) Zhao, Y.; Truhlar, D. G. *Org. Lett.* **2006**, *8*, 5753; (d) Wodrich, M. D.; Corminboeuf, C.; Schereiner, P. R.; Fokin, A. A.; Schleyer, P. v. R. *Org. Lett.* **2007**, *9*, 1851; (e) Schreiner, P. R. *Angew. Chem., Int. Ed.* **2007**, *46*, 4217; (f) Zhao, Y.; Truhlar, D. G. *Acc. Chem. Res.* **2008**, *41*, 157.